Electronic Supplementary Information

Formation of thiolate-bridged diiron complexes featuring anionic isocyanide originating from the activation of counterions in the outer sphere

Sunlin Xu,[a] Dawei Yang,*[a] Jinfeng Zhao,[a] Baomin Wang,[a] and Jingping Qu*[a]

[a]*State Key Laboratory of Fine Chemicals, Dalian University of Technology, 2 Linggong Road, Dalian 116024, P. R. China*

*E-mail: qujp@dlut.edu.cn (J.Q.)

yangdw@dlut.edu.cn (D.Y.)

Contents:

I. X-ray crystallographic data

Table S1. Crystallographic data for **2** and **3**.

	2	**3**
Formula	$C_{27}H_{43}F_6Fe_2N_2PS_2$	$C_{26}H_{39}Fe_2N_2S_2$
Formula weight	716.42	555.41
Crystal dimensions (mm^3)	0.4 × 0.3 × 0.2	0.4 × 0.3 × 0.3
Crystal system	Monoclinic	Monoclinic
Space group	$P2_1/m$	$P2_1/c$
a (Å)	9.197(3)	10.6910(8)
b (Å)	16.209(4)	14.4262(11)
c (Å)	10.954(3)	17.5493(13)
α (°)	90	90
β (°)	90.286(4)	94.3180(10)
γ (°)	90	90
Volume ($Å^3$)	1632.9(8)	2699.0(4)
Z	2	4
T (K)	300.13	300.16
D_{calcd} (g cm^{-3})	1.457	1.367
μ (mm^{-1})	1.119	1.246
F (000)	744.0	1172.0
No. of rflns. collected	24159	33469
No. of indep. rflns. / R_{int}	3090 / 0.0457	6195 / 0.0547
No. of obsd. rflns. [$I_0 > 2\sigma(I_0)$]	2866	4566
Data / restraints / parameters	3090 / 0 / 208	6195 / 1 / 312
R_1 / wR_2 [$I_0 > 2\sigma(I_0)$]	0.0312 / 0.0730	0.0393 / 0.0869
R_1 / wR_2 (all data)	0.0368 / 0.0769	0.0651 / 0.0970
GOF (on F^2)	1.132	1.017
Largest diff. peak and hole (e $Å^{-3}$)	0.268/ −0.460	0.428 / −0.327
CCDC No.	2098968	2098969

Table S2. Crystallographic data for **4** and **5**.

	4	**5**
Formula	$C_{29}H_{48}F_{11}Fe_2N_2P_2S_2Si$	$C_{26}H_{40}F_{10}Fe_2N_2P_2S_2$
Formula weight	899.54	808.36
Crystal dimensions (mm^3)	0.4 × 0.3 × 0.2	0.2 × 0.2 × 0.1
Crystal system	Orthorhombic	Monoclinic
Space group	*Pbca*	*C2/c*
a (Å)	17.0907(10)	10.479(3)
b (Å)	15.7948(9)	19.104(5)
c (Å)	32.7765(18)	17.747(5)
α (°)	90	90
β (°)	90	105.836(6)
γ (°)	90	90
Volume ($Å^3$)	8847.8(9)	3417.9(17)
Z	8	4
T (K)	173.0	298.0
D_{calcd} (g cm^{-3})	1.351	1.571
μ (mm^{-1})	0.917	1.140
F (000)	3704.0	1656.0
No. of rflns. collected	40160	8048
No. of indep. rflns. / R_{int}	7855 / 0.0678	3108 / 0.0245
No. of obsd. rflns. [$I_0 > 2\sigma(I_0)$]	4966	2502
Data / restraints / parameters	7855 / 361 / 619	3108 / 66 / 224
R_1 / wR_2 [$I_0 > 2\sigma(I_0)$]	0.0648 / 0.1579	0.0445 / 0.1092
R_1 / wR_2 (all data)	0.1156/ 0.1830	0.0586 / 0.1195
GOF (on F^2)	1.024	1.040
Largest diff. peak and hole (e $Å^{-3}$)	0.596 / −0.487	0.487 / −0.563
CCDC No.	2083465	2083463

Table S3. Crystallographic data for **6** and **7**.

	6	**7**
Formula	$C_{44}H_{55}BF_5Fe_2N_2PS_2$	$C_{33}H_{50}F_{11}Fe_2N_3P_2S_2$
Formula weight	924.50	935.52
Crystal dimensions (mm^3)	0.4 ×0.2 ×0.2	0.4 ×0.4 ×0.3
Crystal system	Triclinic	Orthorhombic
Space group	*P*1	*Pnma*
a (Å)	10.1726(6)	20.6464(13)
b (Å)	11.9179(7)	12.2863(8)
c (Å)	18.6830(11)	18.6507(12)
α (°)	97.2170(10)	90
β (°)	97.8230(10)	90
γ (°)	103.6040(10)	90
Volume ($Å^3$)	2151.6(2)	4731.1(5)
Z	2	4
T (K)	173.0	233.0
D_{calcd} ($g\ cm^{-3}$)	1.427	1.313
μ (mm^{-1})	0.864	0.837
F (000)	964.0	1928.0
No. of rflns. collected	42504	23032
No. of indep. rflns. / R_{int}	17536 / 0.0541	4021 / 0.0267
No. of obsd. rflns. [$I_0 > 2\sigma(I_0)$]	13772	3510
Data / restraints / parameters	17536/ 4 / 1052	4021/ 12 / 285
R_1 / wR_2 [$I_0 > 2\sigma(I_0)$]	0.0498 / 0.0842	0.0513 / 0.1334
R_1 / wR_2 (all data)	0.0773 / 0.0915	0.0580 / 0.1412
GOF (on F^2)	1.016	1.026
Largest diff. peak and hole (e $Å^{-3}$)	0.530 / −0.386	1.402/ −0.534
CCDC No.	2083466	2083464

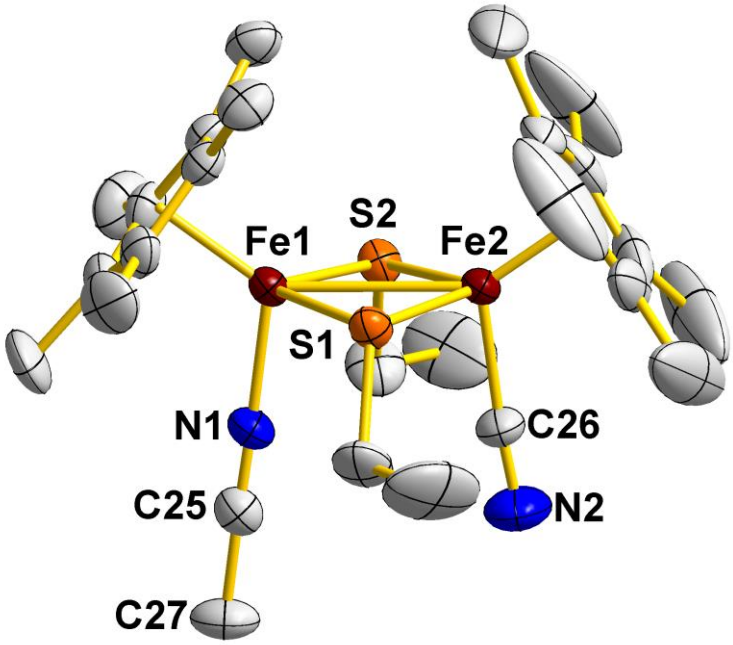

Figure S1. ORTEP diagram of **2**.

The thermal ellipsoids are shown at a 50% probability level. All hydrogen atoms and counter anion PF_6^- are omitted for clarity.

Table S4. Selected bond distances (Å) and angles (°) for **2**.

Distances (Å)			
Fe1–Fe2	2.7533(11)	Fe1–S1	2.2132(10)
Fe1–S2	2.2132(10)	Fe2–S1	2.2209(10)
Fe2–S2	2.2209(10)	Fe1–N1	1.912(4)
N1–C25	1.123(6)	Fe2–C26	1.893(5)
C26–N2	1.116(7)		
Angles (°)			
Fe1–S1–Fe2	76.77(3)	Fe1–S2–Fe2	76.77(3)
Fe1–N1–C25	178.6(4)	Fe2–C26–N2	176.1(5)
Torsion angles (°)			
S1–Fe1Fe2–S2	7.5(5)		
Dihedral angles (°)			
Cp*1^Cp*2	69.1(1)		

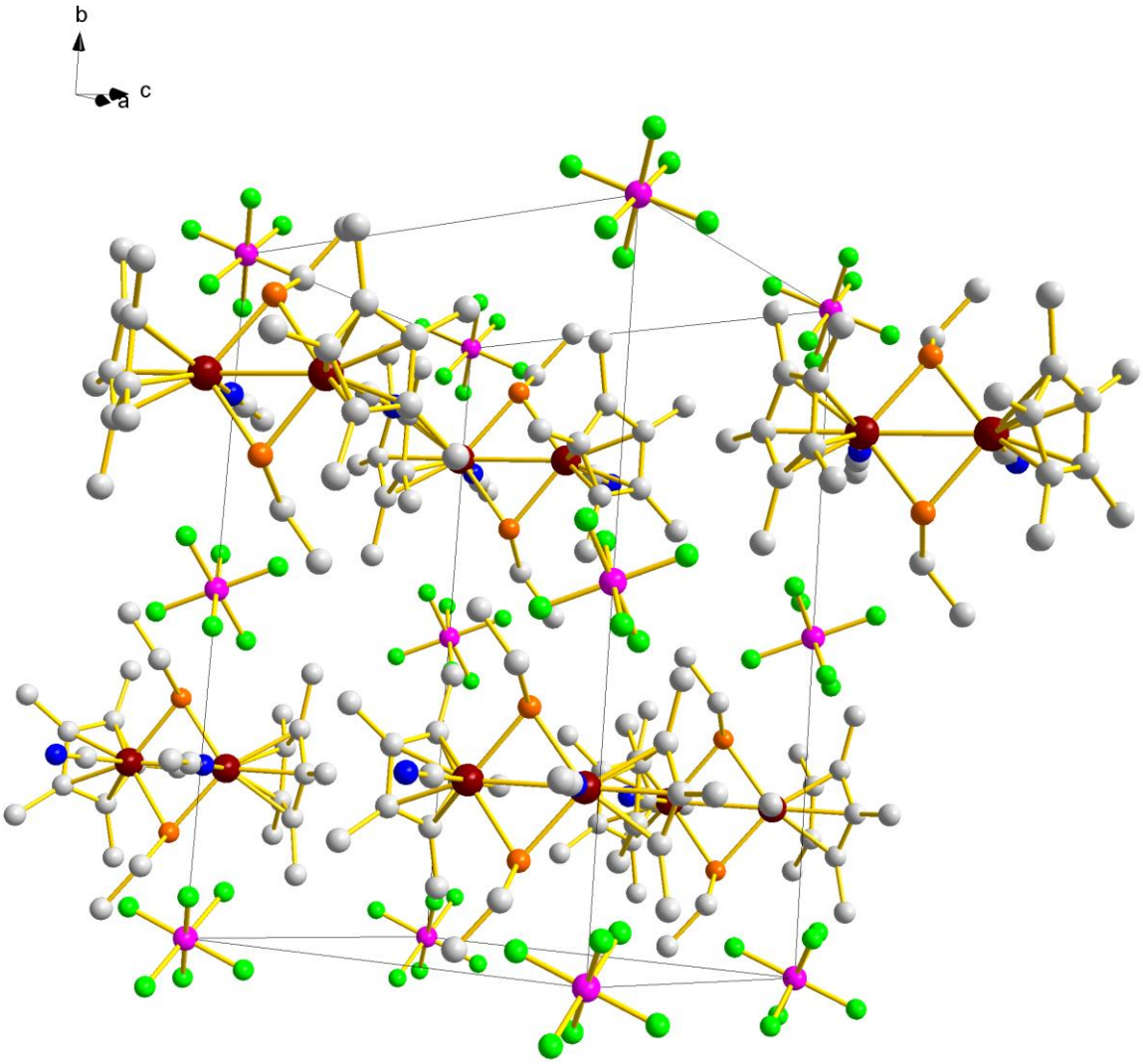

Figure S2. Crystal packing diagram of **2**.

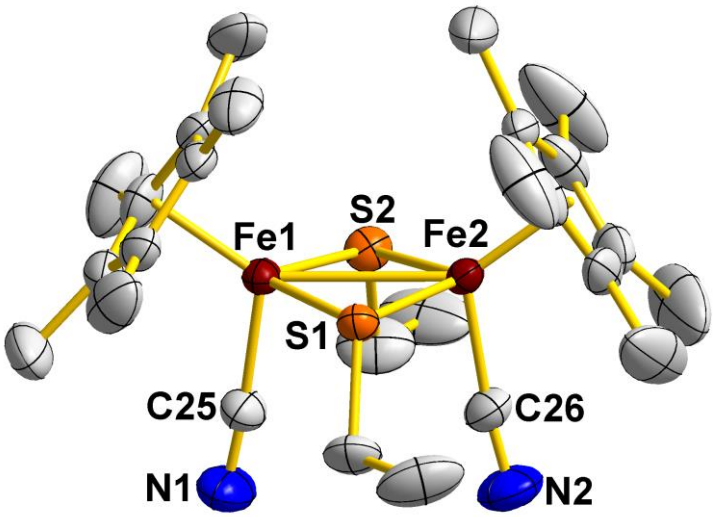

Figure S3. ORTEP diagram of **3**.

The thermal ellipsoids are shown at a 50% probability level. All hydrogen atoms are omitted for clarity.

Table S5. Selected bond distances (Å) and angles (°) for **3**.

Distances (Å)			
Fe1–Fe2	2.7479(5)	Fe1–S1	2.2042(7)
Fe1–S2	2.2042(8)	Fe2–S1	2.2048(7)
Fe2–S2	2.2148(8)	Fe1–C25	1.902(3)
C25–N1	1.143(4)	Fe2–C26	1.903(3)
C26–N2	1.145(4)		
Angles (°)			
Fe1–S1–Fe2	77.11(2)	Fe1–S2–Fe2	76.90(3)
Fe1–C25–N1	175.9(3)	Fe2–C26–N2	174.3(3)
Torsion angles (°)			
S1–Fe1Fe2–S2	9.1(3)		
Dihedral angles (°)			
Cp*1^Cp*2	68.9(1)		

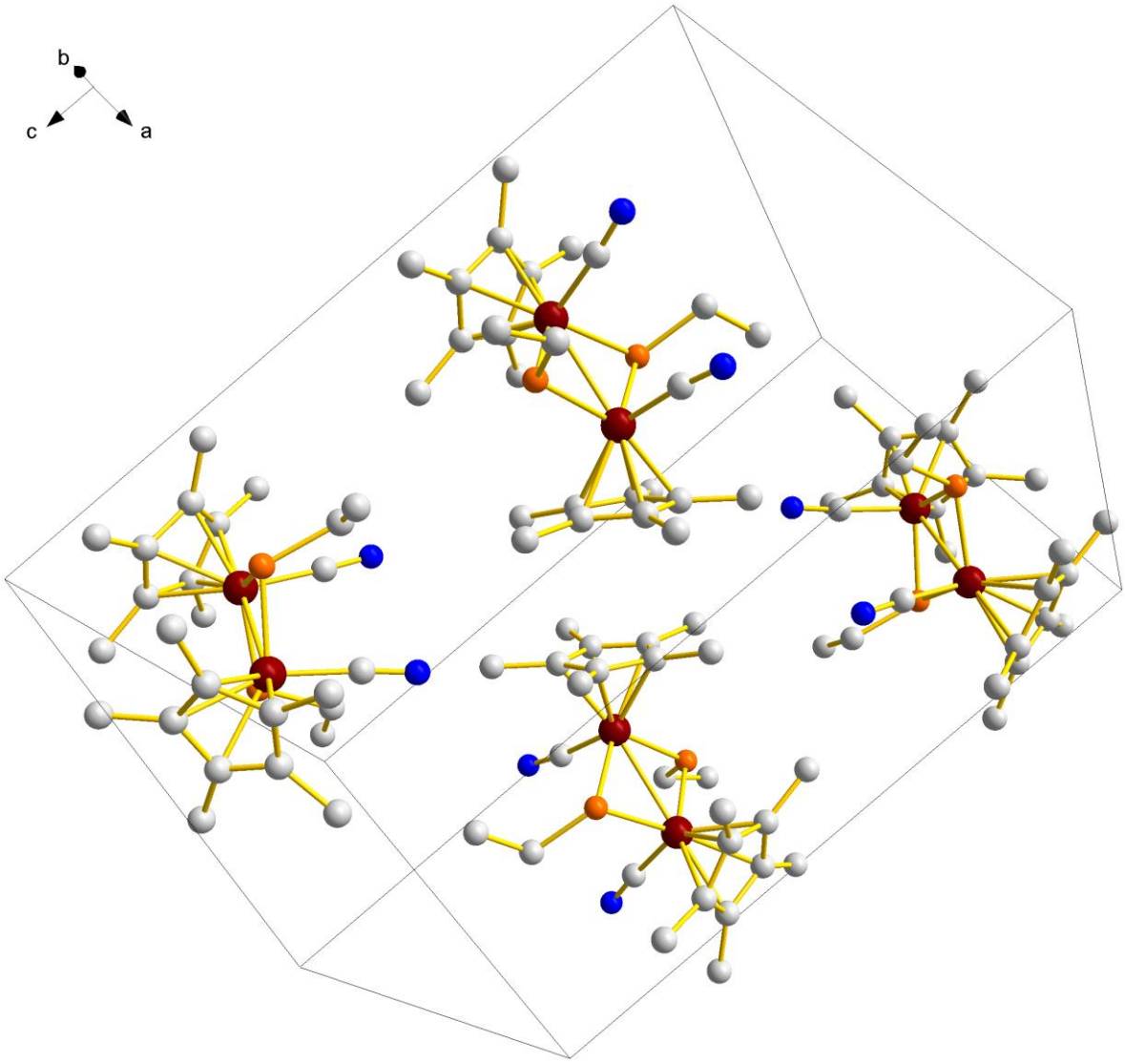

Figure S4. Crystal packing diagram of **3**.

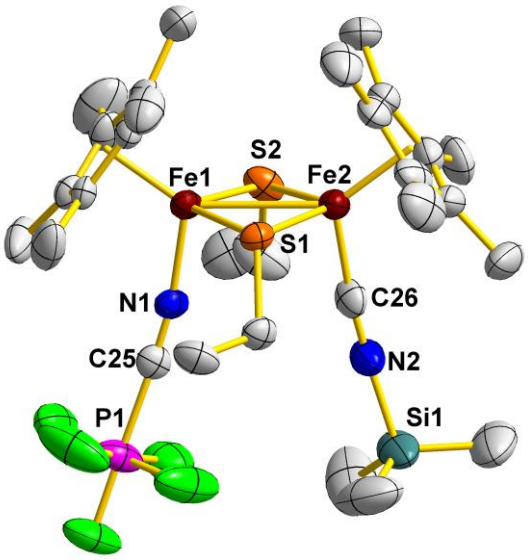

Figure S5. ORTEP diagram of **4**.

The thermal ellipsoids are shown at a 50% probability level. All hydrogen atoms and counter anion PF_6^- are omitted for clarity

Table S6. Selected bond distances (Å) and angles (°) for **4**.

Distances (Å)			
Fe1–Fe2	2.7441(10)	Fe1–S1	2.2165(14)
Fe1–S2	2.2223(18)	Fe2–S1	2.2167(15)
Fe2–S2	2.2134(16)	Fe1–N1	1.914(5)
N1–C25	1.146(7)	C25–P1	1.867(6)
Fe2–C26	1.827(6)	C26–N2	1.171(7)
N2–Si1	1.802(6)		
Angles (°)			
Fe1–S1–Fe2	76.48(5)	Fe1–S2–Fe2	76.43(5)
Fe1–N1–C25	170.8(5)	N1–C25–P1	176.1(5)
Fe2–C26–N2	174.3(5)	C26–N2–Si1	170.8(6)
Torsion angles (°)			
S1–Fe1Fe2–S2	7.4(6)		
Dihedral angles (°)			
Cp*1^Cp*2	72.7(5)		

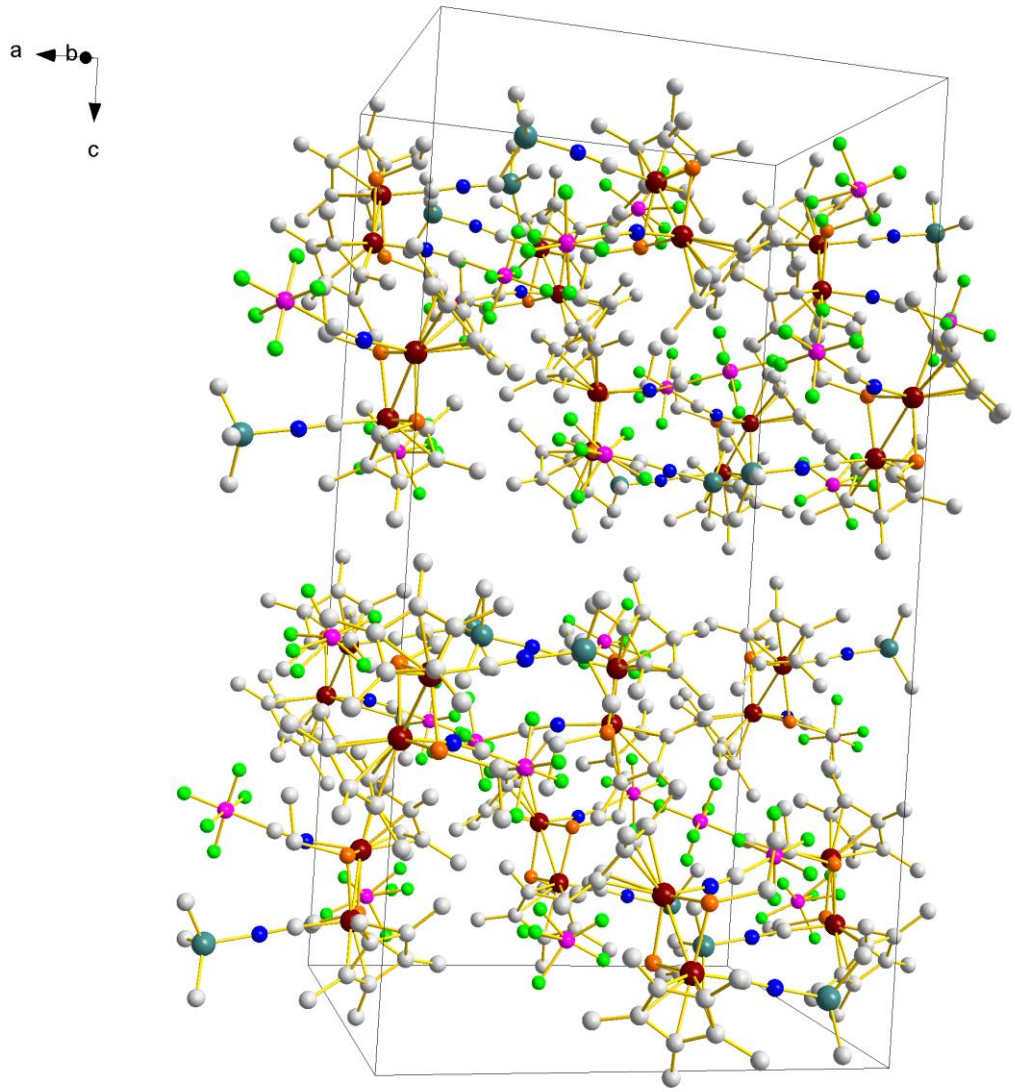

Figure S6. Crystal packing diagram of **4**.

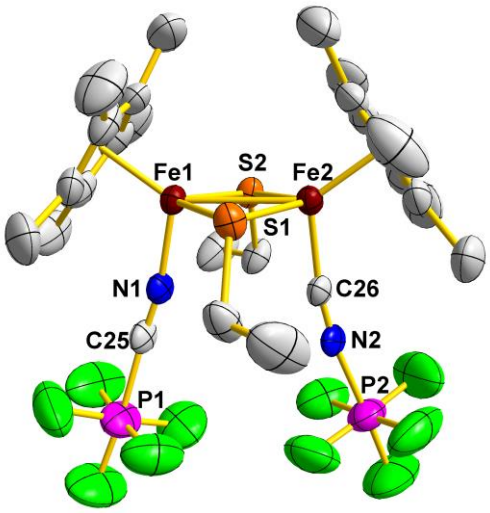

Figure S7. ORTEP diagram of **5**.

The thermal ellipsoids are shown at a 50% probability level. All hydrogen atoms are omitted for clarity.

Table S7. Selected bond distances (Å) and angles (°) for **5**.

Distances (Å)			
Fe1–Fe2	2.7596(11)	Fe1–S1	2.2221(11)
Fe1–S2	2.2221(11)	Fe2–S1	2.2219(11)
Fe2–S2	2.2219(11)	Fe1–N1	1.899(9)
C25–N1	1.129(10)	C25–P1	1.856(10)
Fe2–C26	1.906(10)	C26–N2	1.133(9)
N2–P2	1.857(8)		
Angles (°)			
Fe1–S1–Fe2	76.77(3)	Fe1–S2–Fe2	76.77(3)
Fe1–N1–C25	169(3)	N1–C25–P1	170.6(18)
Fe2–C26–N2	171(3)	C26–N2–P2	172(2)
Torsion angles (°)			
S1–Fe1Fe2–S2	7.2(6)		
Dihedral angles (°)			
Cp*1^Cp*2	67.2(6)		

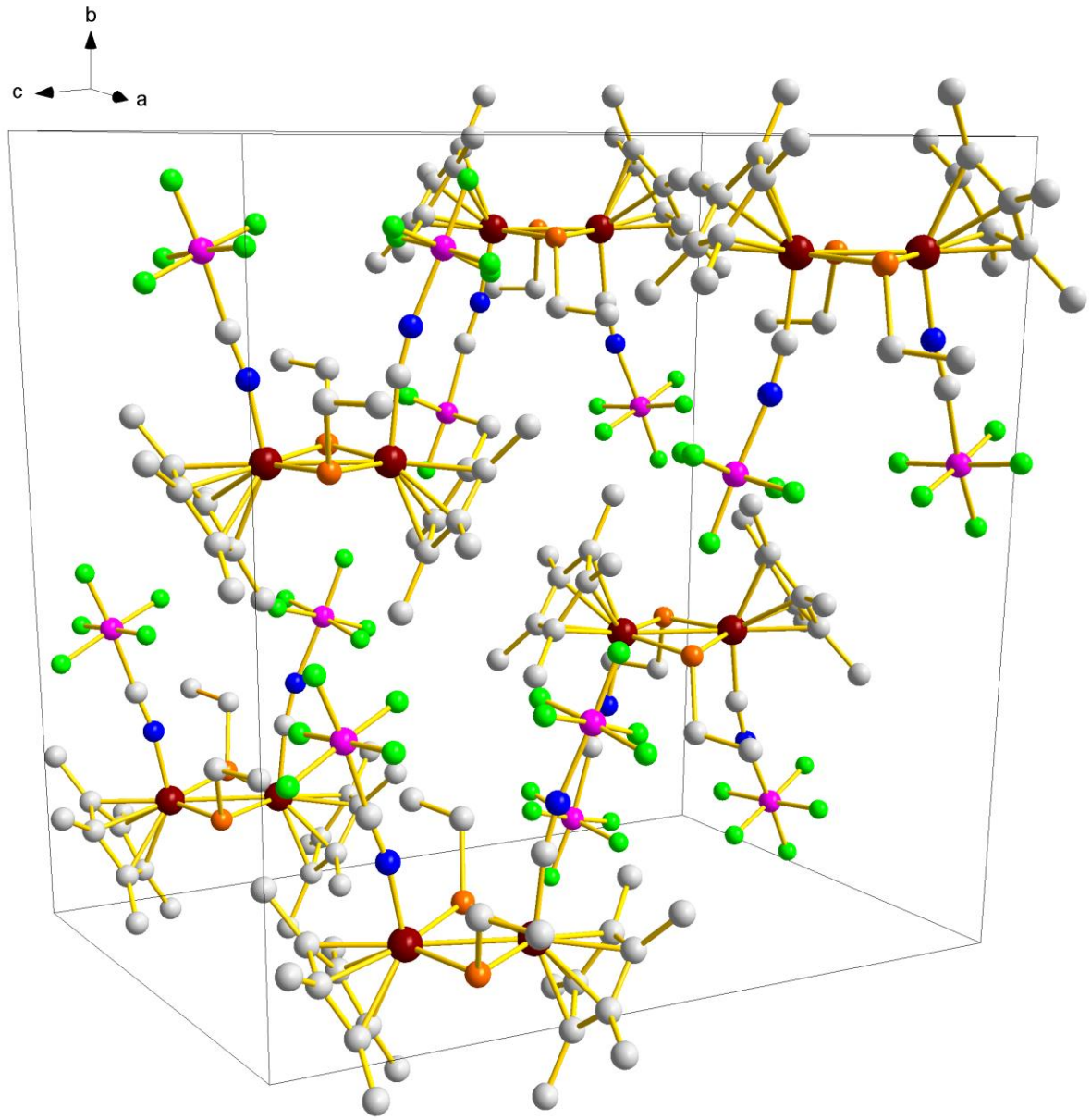

Figure S8. Crystal packing diagram of **5**.

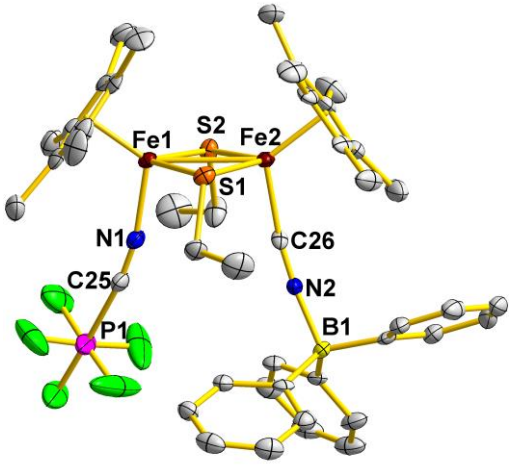

Figure S9. ORTEP diagram of **6**.

The thermal ellipsoids are shown at a 50% probability level. All hydrogen atoms are omitted for clarity.

Table S8. Selected bond distances (Å) and angles (°) for **6**.

Distances (Å)			
Fe1–Fe2	2.7572(11)	Fe1–S1	2.2230(18)
Fe1–S2	2.2112(17)	Fe2–S1	2.2091(18)
Fe2–S2	2.2198(18)	Fe1–N1	1.931(5)
N1–C25	1.136(7)	C25–P1	1.895(7)
Fe2–C26	1.911(6)	C26–N2	1.152(7)
N2–B1	1.618(8)		
Angles (°)			
Fe1–S1–Fe2	76.94(6)	Fe1–S2–Fe2	76.96(6)
Fe1–N1–C25	166.4(5)	N1–C25–P1	169.3(6)
Fe2–C26–N2	170.6(5)	C26–N2–B1	173.5(5)
Torsion angles (°)			
S1–Fe1Fe2–S2	5.2(5)		
Dihedral angles (°)			
Cp*1^Cp*2	71.3(2)		

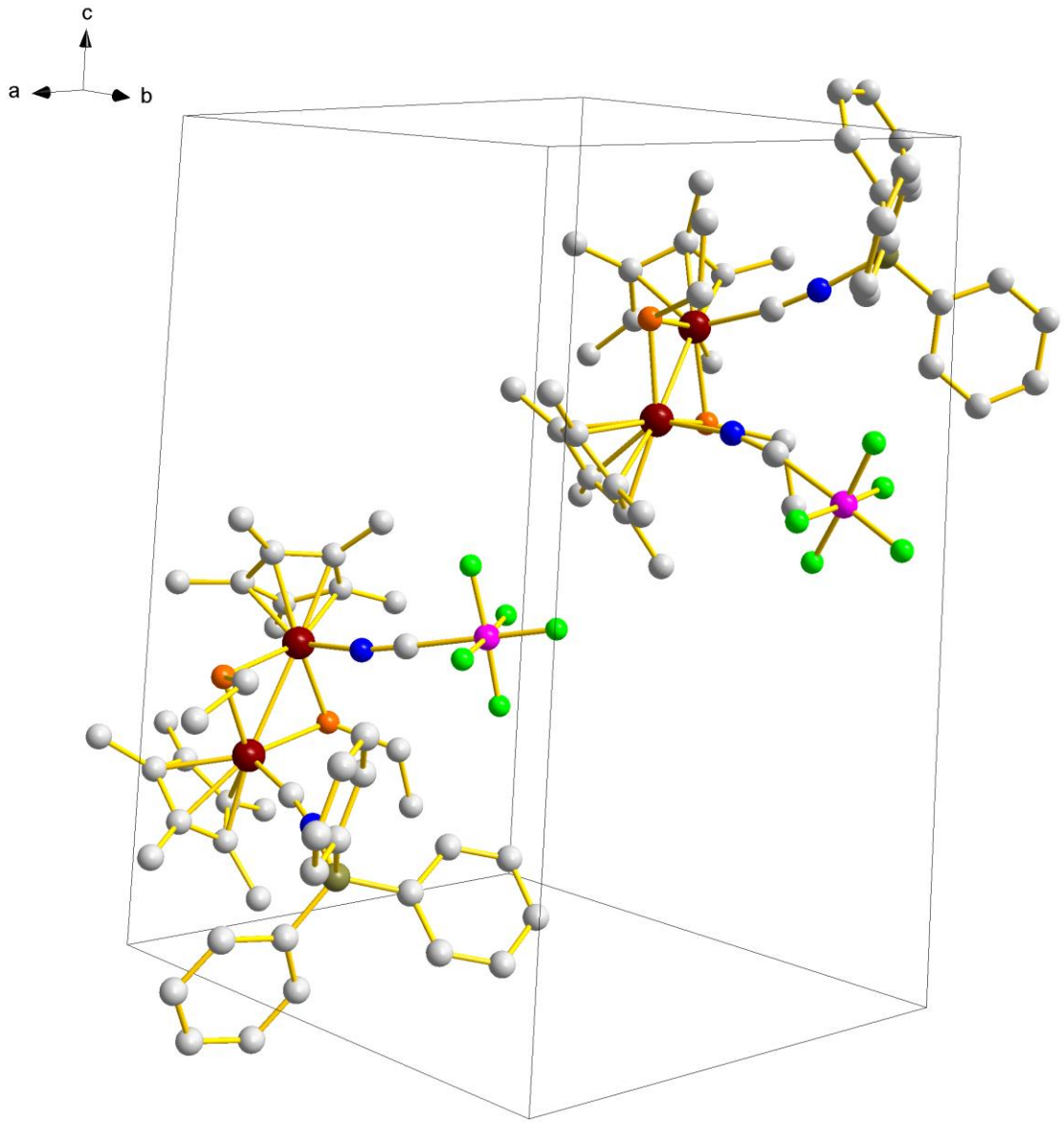

Figure S10. Crystal packing diagram of **6**.

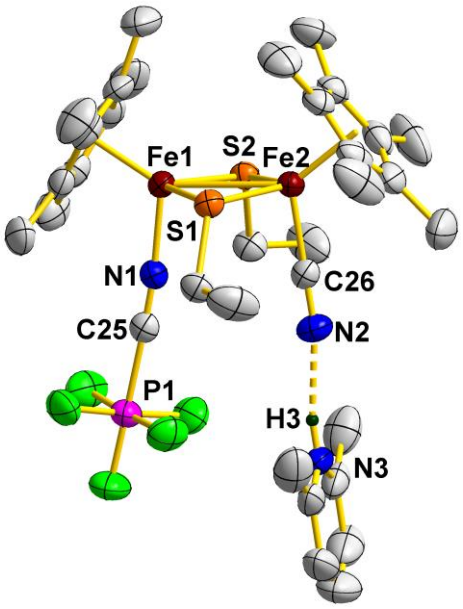

Figure S11. ORTEP diagram of **7**.

The thermal ellipsoids are shown at a 50% probability level. All hydrogen atoms except for 2,6-dimethylpyridine group and counter anion PF_6^- are omitted for clarity.

Table S9. Selected bond distances (Å) and angles (°) for **7**.

Distances (Å)			
Fe1–Fe2	2.7449(9)	Fe1–S1	2.2314(9)
Fe1–S2	2.2163(9)	Fe2–S1	2.2314(9)
Fe2–S2	2.2163(9)	Fe1–N1	1.909(4)
N1–C25	1.136(6)	C25–P1	1.863(5)
Fe2–C26	1.894(5)	C26–N2	1.153(6)
Angles (°)			
Fe1–S1–Fe2	76.22(3)	Fe1–S2–Fe2	76.22(3)
Fe1–N1–C25	174.6(4)	N1–C25–P1	178.3(4)
Fe2–C26–N2	179.6(4)		
Torsion angles (°)			
S1–Fe1Fe2–S2	7.4(5)		
Dihedral angles (°)			
Cp*1^Cp*2	68.1(2)		

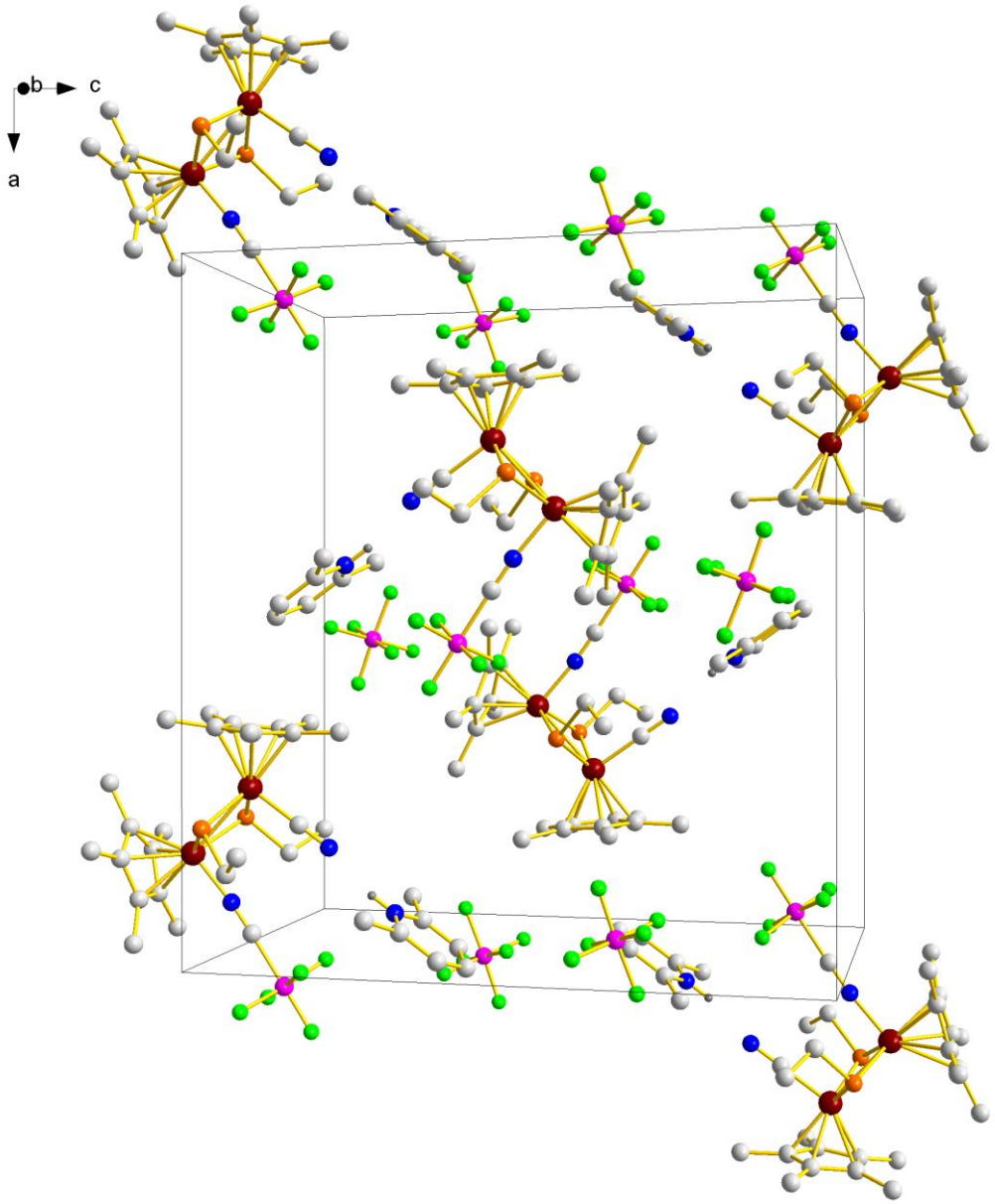

Figure S12. Crystal packing diagram of **7**.

II. ESI high resolution mass spectra

(a)

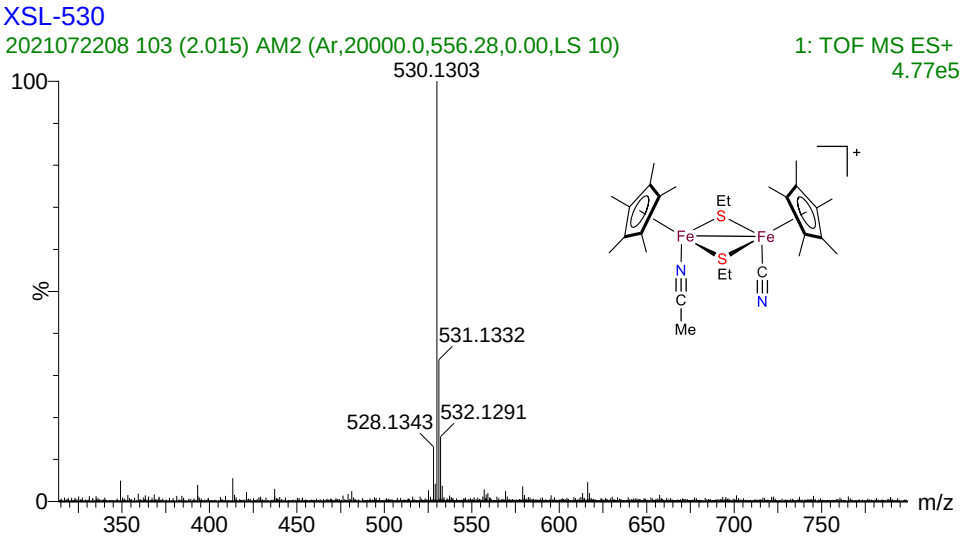

(b)

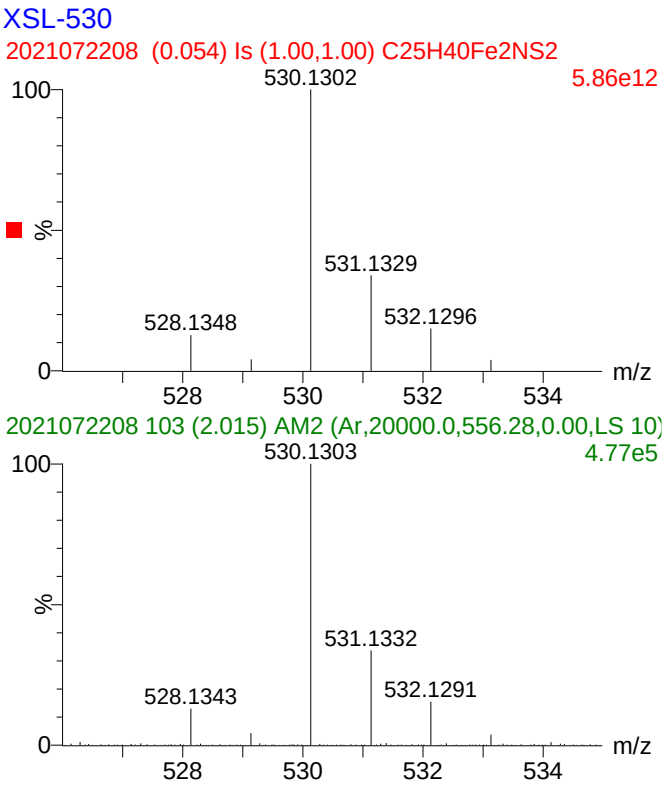

Figure S13. High resolution mass spectrum of **2** in CH_2Cl_2.

(a) The signal at *m*/*z* 530.1303 corresponds to $[\mathbf{2}–MeCN–PF_6]^+$. (b) Calculated isotopic distribution for $[\mathbf{2}–PF_6]^+$ (upper) and the amplifying experimental diagram for $[\mathbf{2}–MeCN–PF_6]^+$ (bottom).

III. NMR spectra

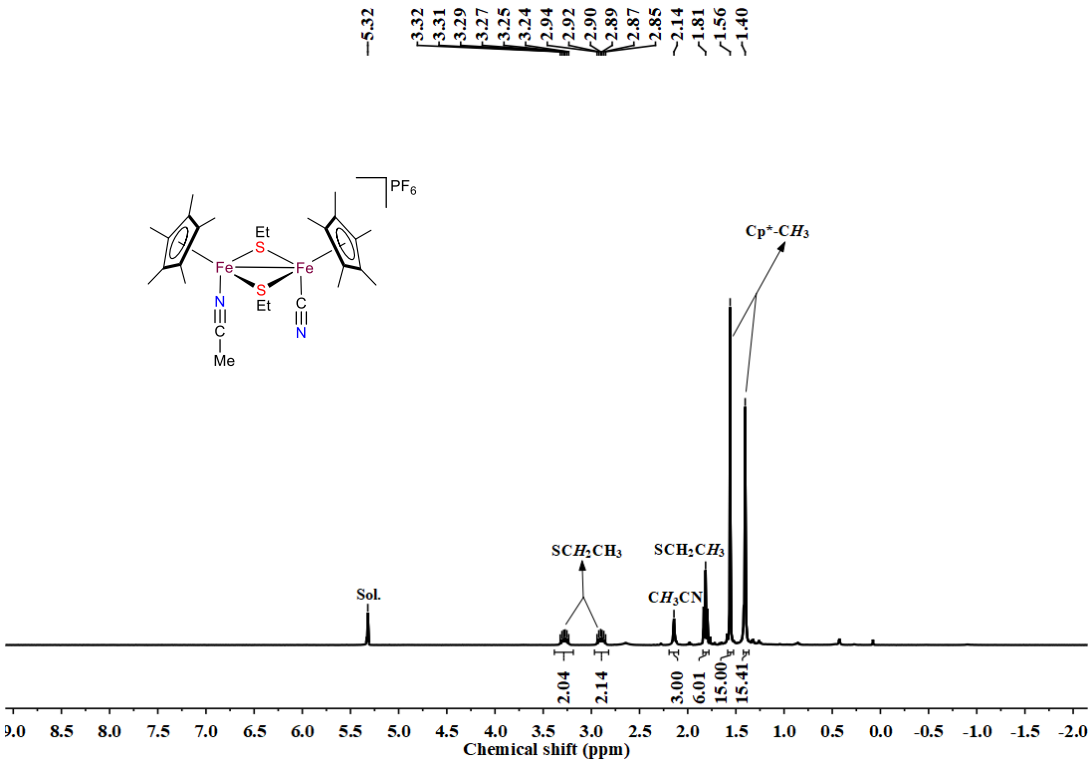

Figure S14. The ^{1}H NMR spectrum of **2** in CD_2Cl_2.

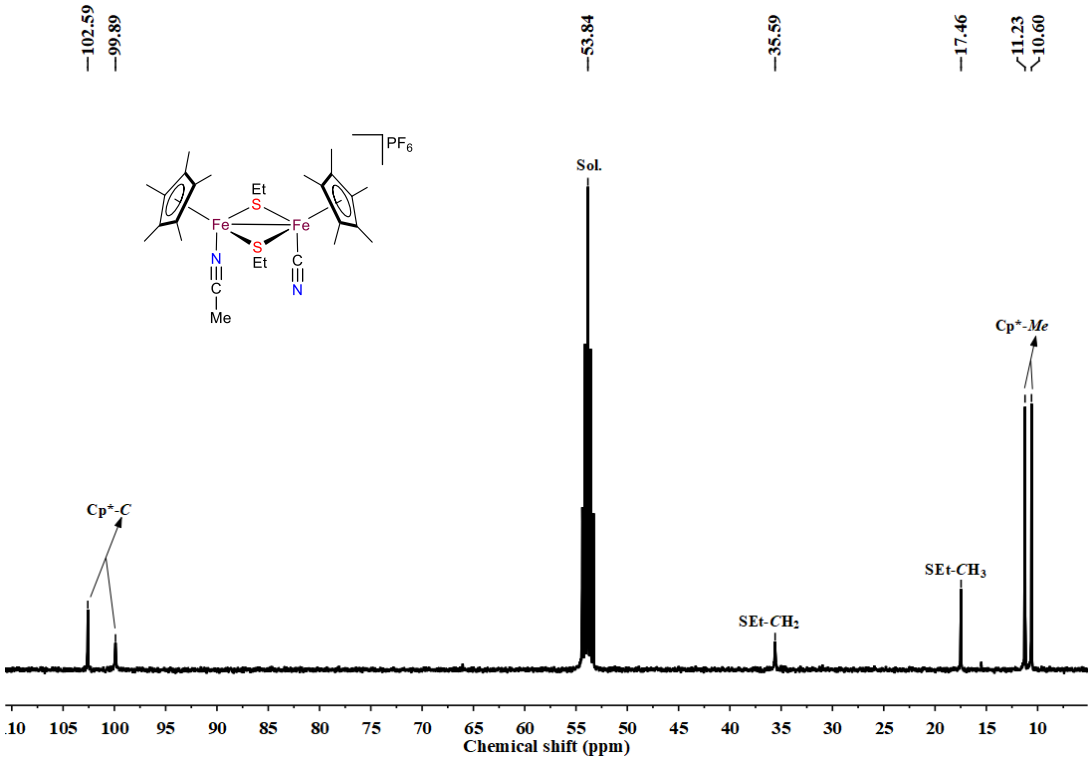

Figure S15. The ^{13}C NMR spectrum of **2** in CD_2Cl_2.

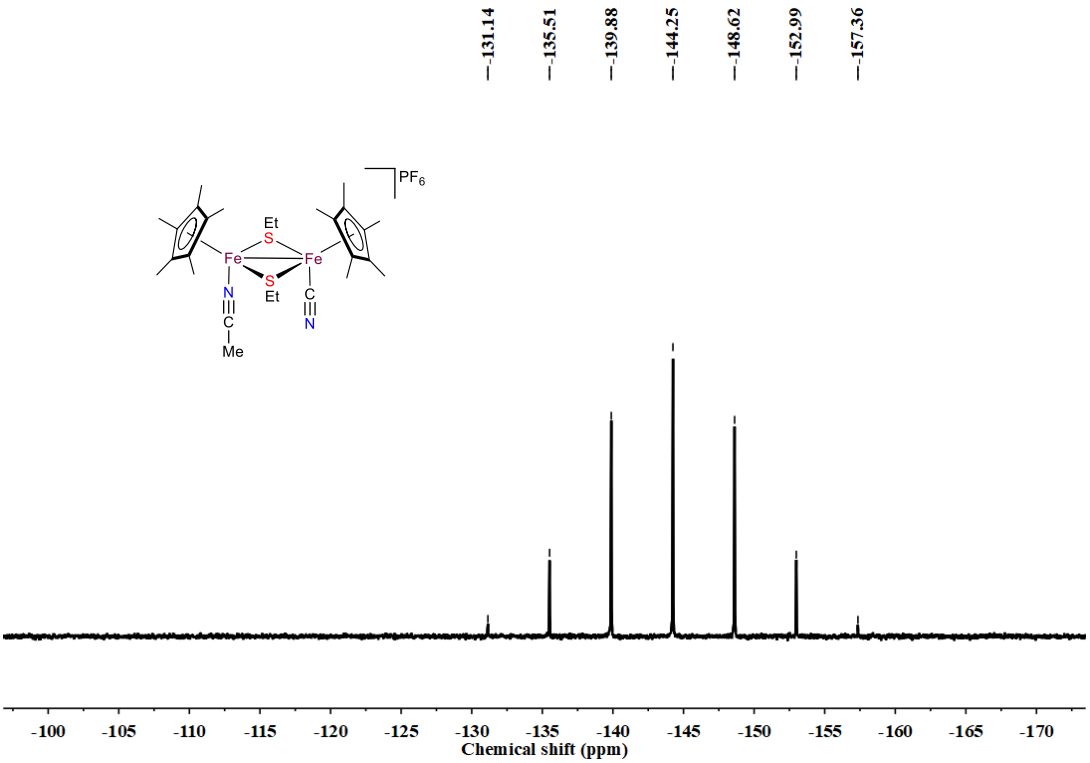

Figure S16. The ^{31}P NMR spectrum of **2** in CD_2Cl_2.

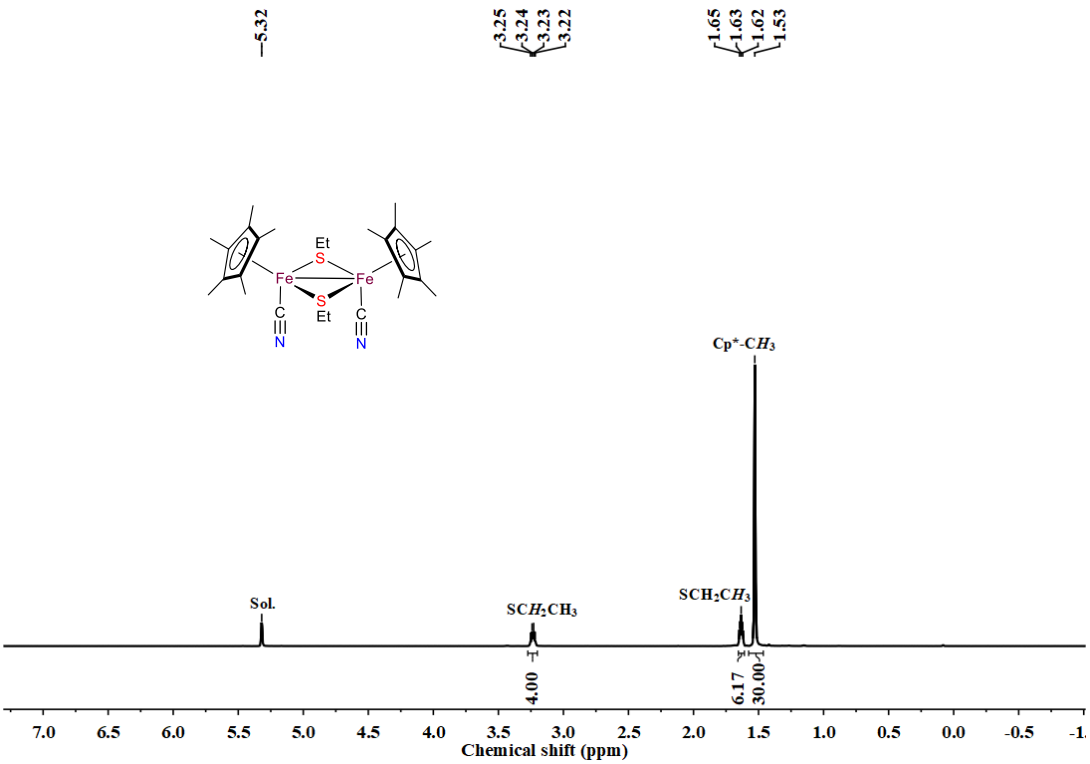

Figure S17. The ^{1}H NMR spectrum of **3** in CD_2Cl_2.

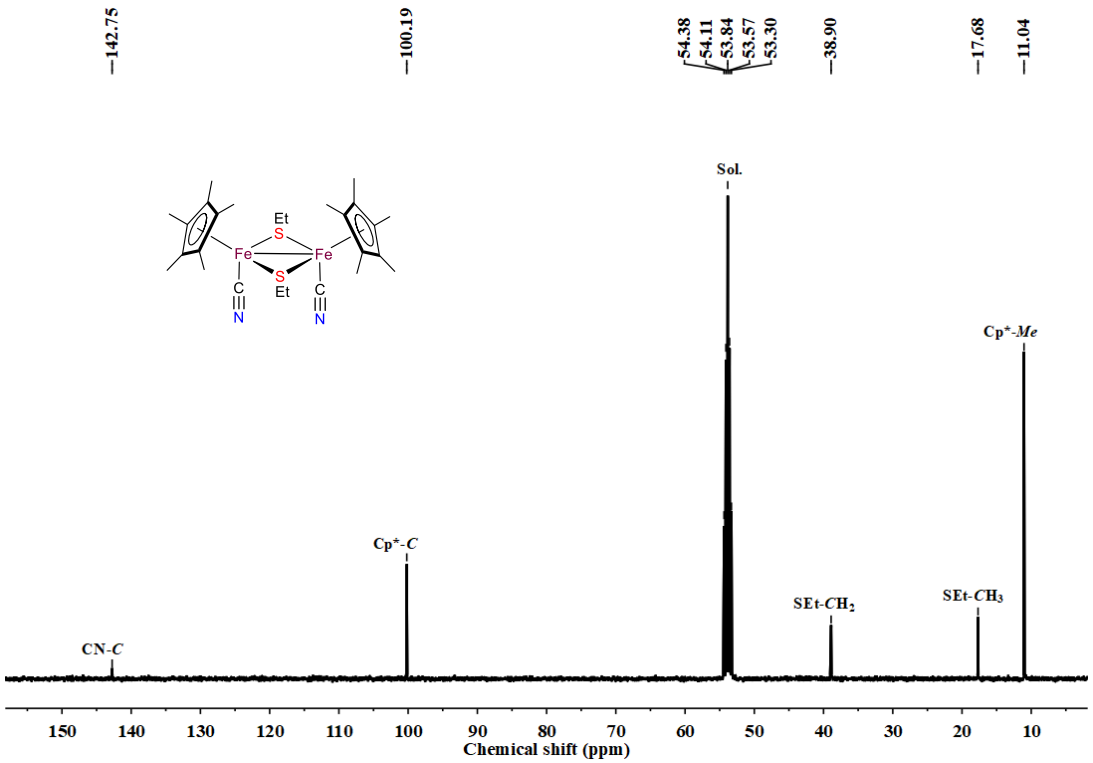

Figure S18. The ^{13}C NMR spectrum of **3** in CD_2Cl_2

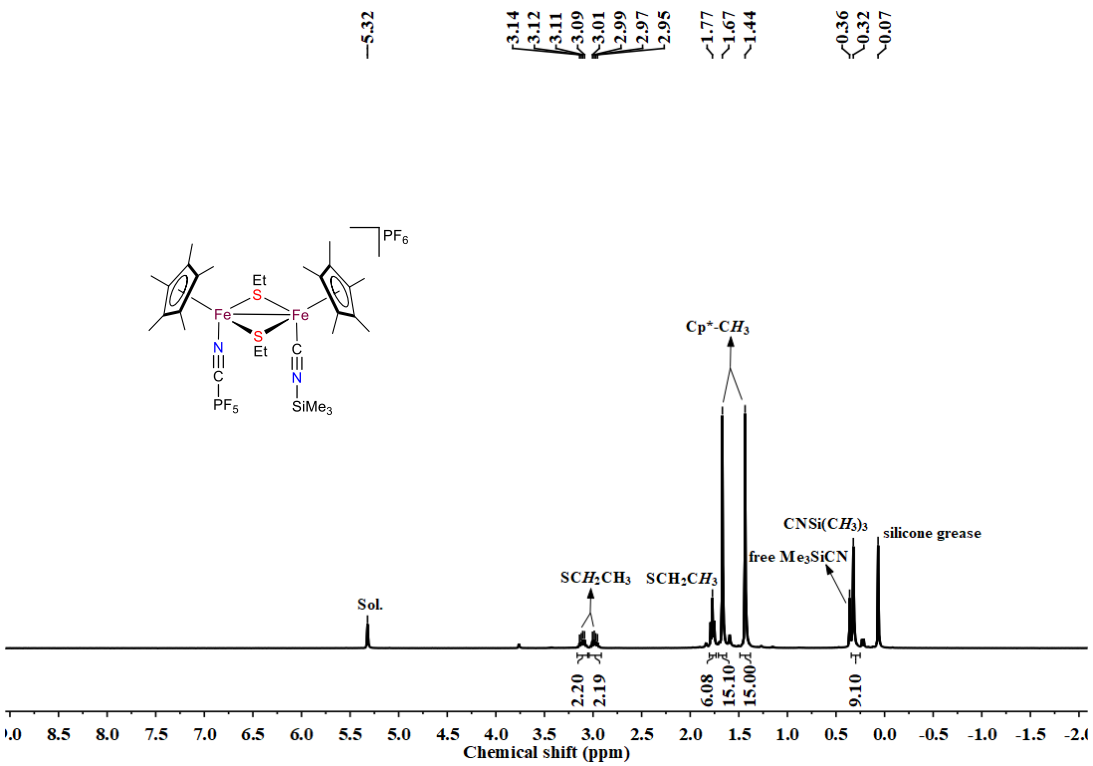

Figure S19. The ^{1}H NMR spectrum of **4** in CD_2Cl_2.

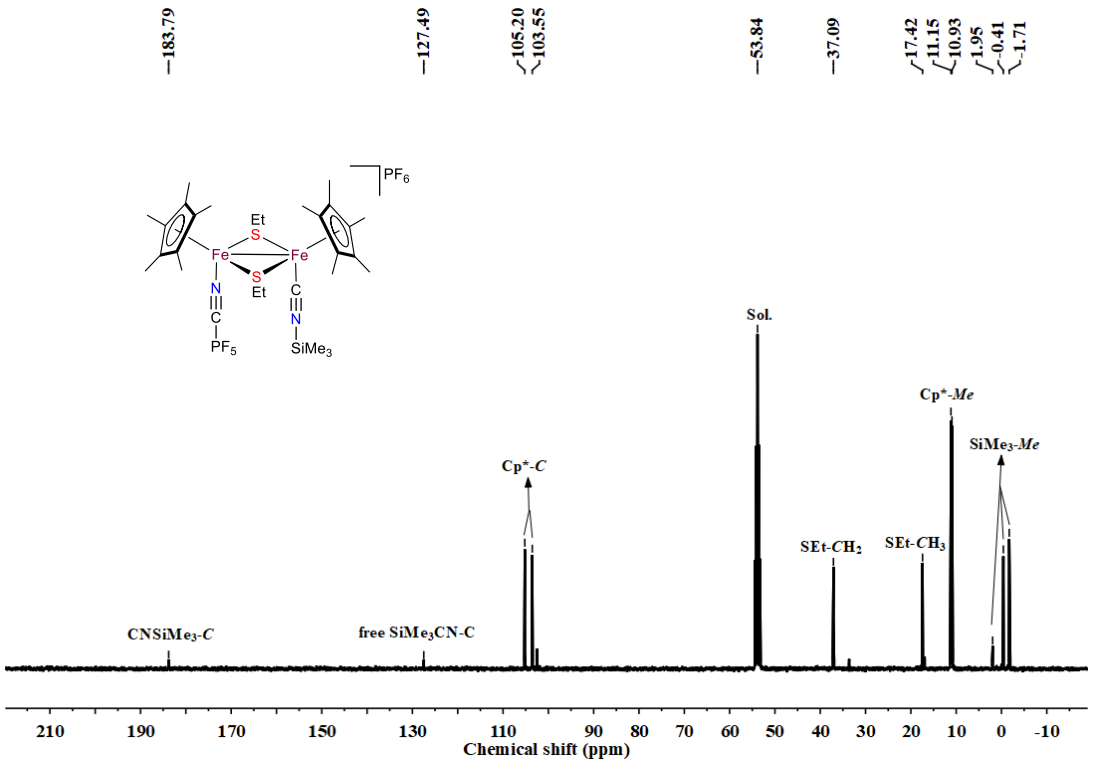

Figure S20. The ^{13}C NMR spectrum of **4** in CD_2Cl_2.

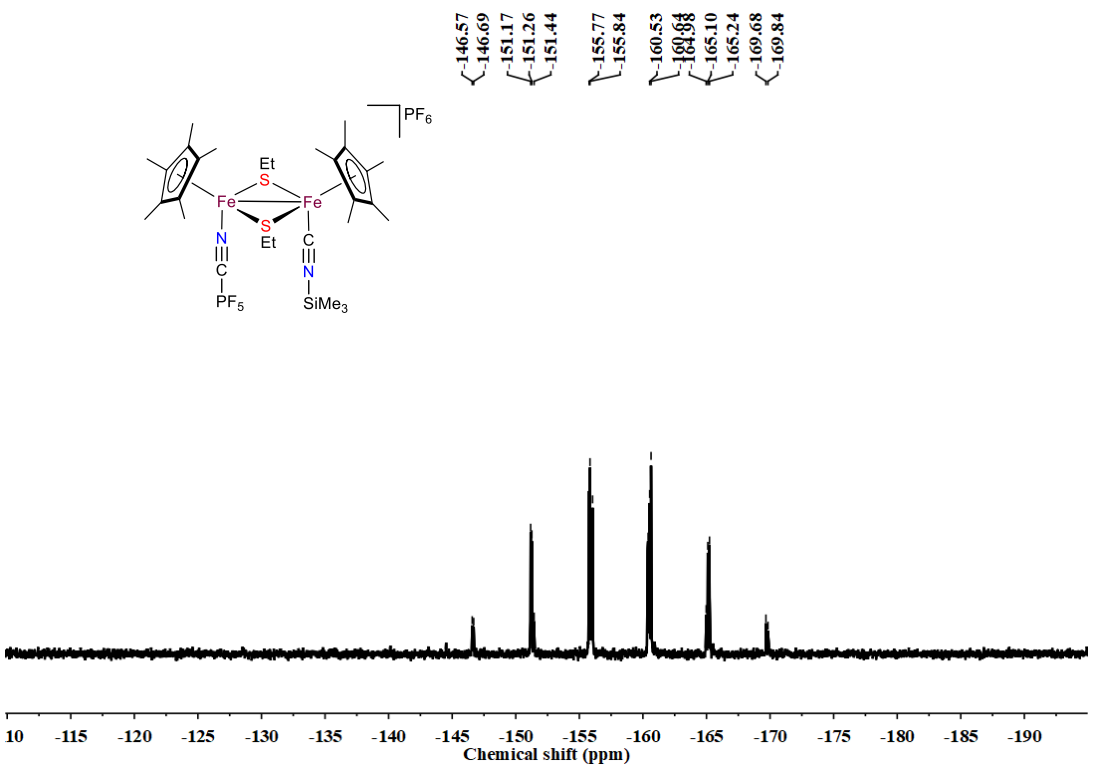

Figure S21. The ^{31}P NMR spectrum of **4** in CD_2Cl_2.

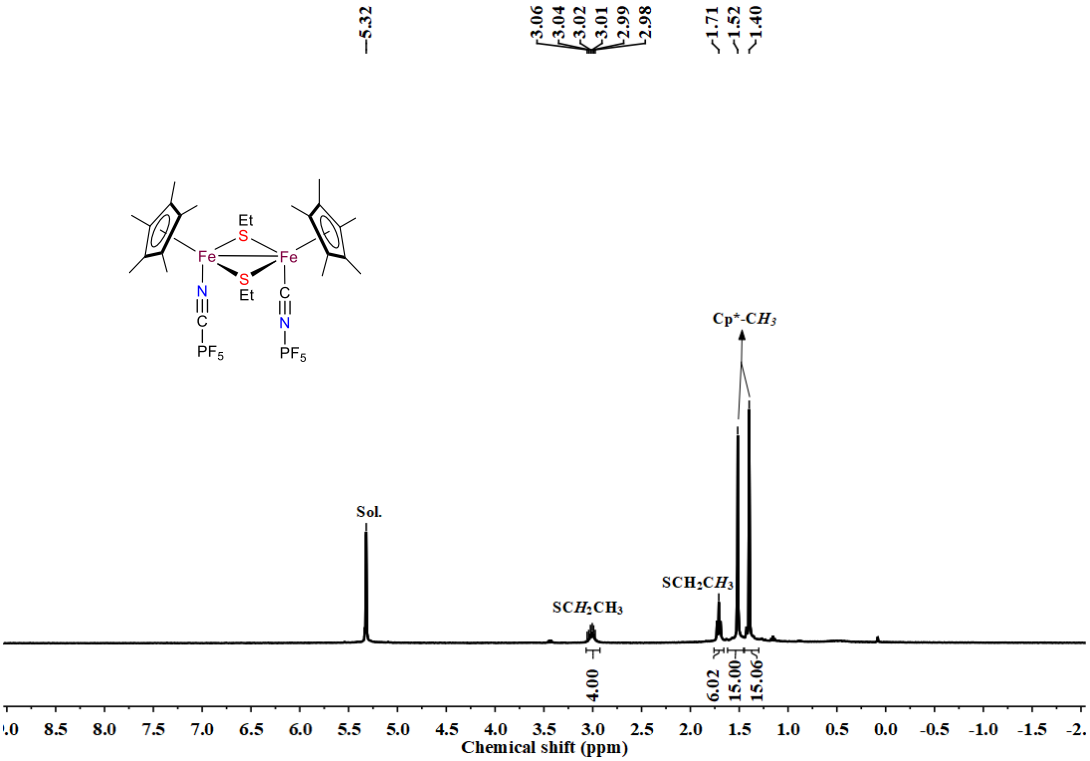

Figure S22. The ^{1}H NMR spectrum of **5** in CD_2Cl_2.

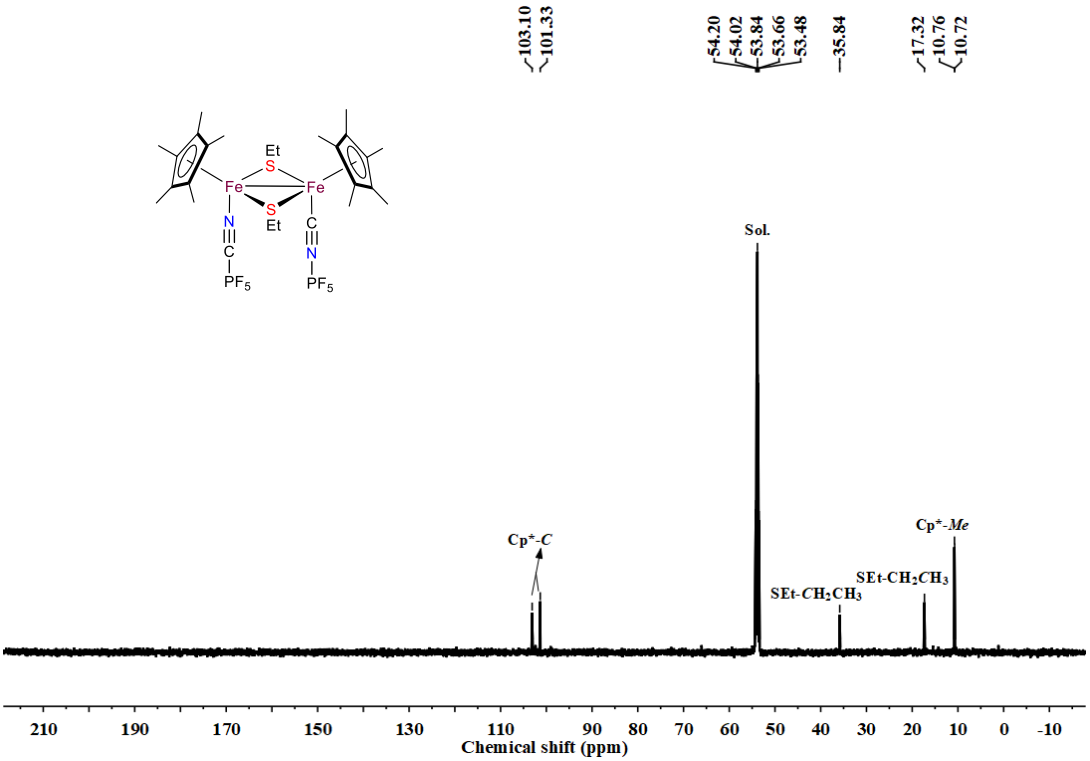

Figure S23. The ^{13}C NMR spectrum of **5** in CD_2Cl_2.

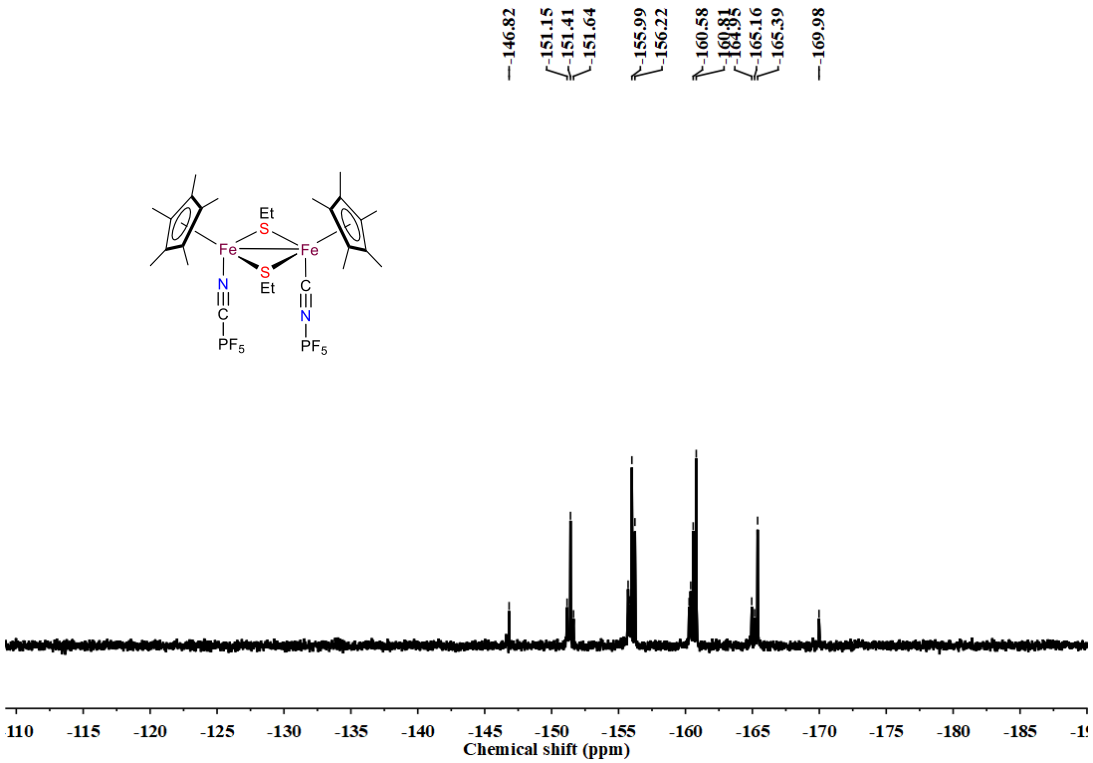

Figure S24. The ^{31}P NMR spectrum of **5** in CD_2Cl_2.

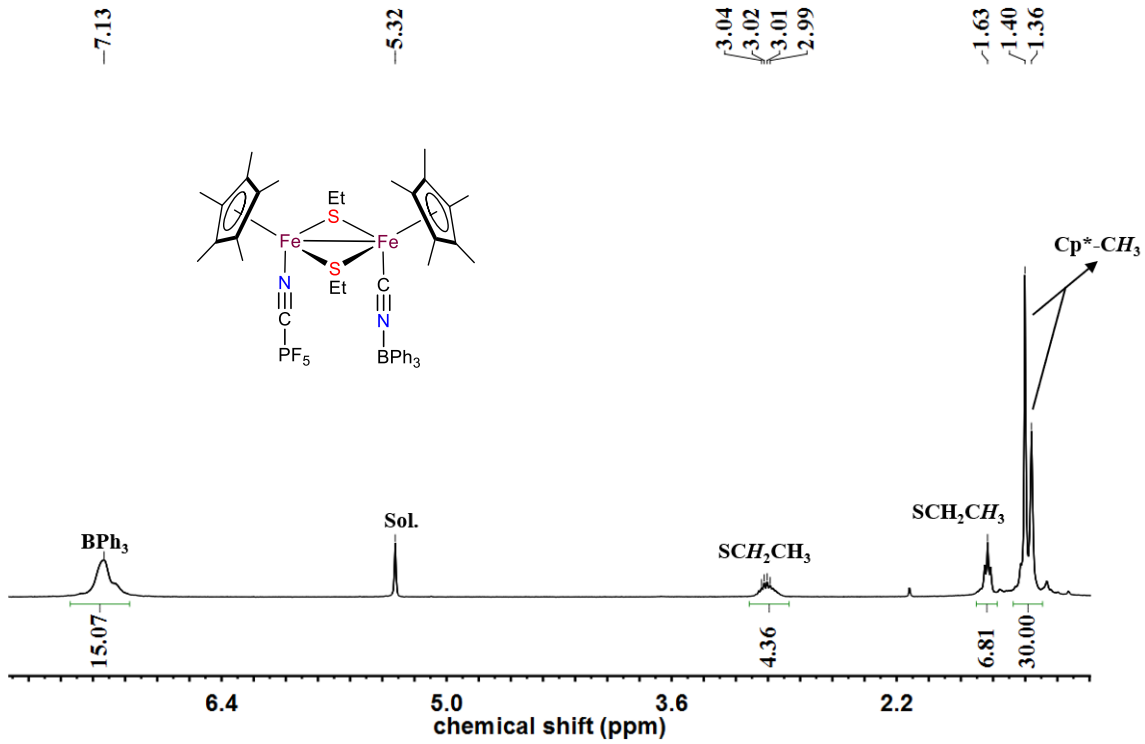

Figure S25. The ^{1}H NMR spectrum of **6** in CD_2Cl_2.

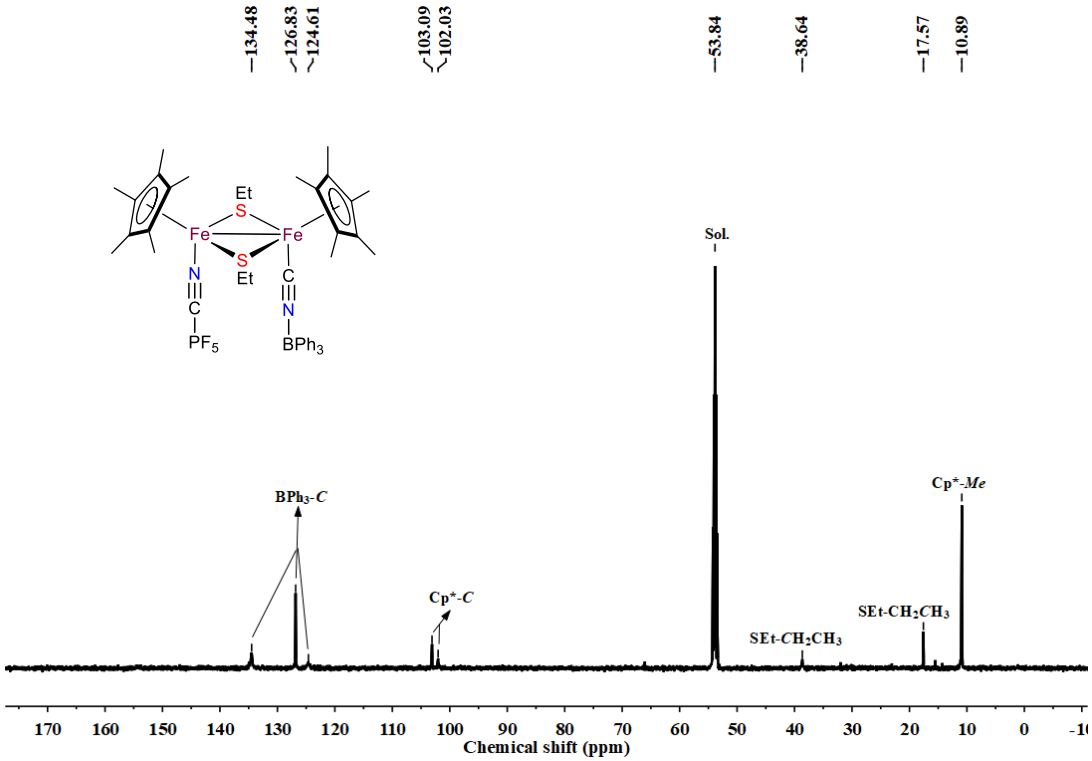

Figure S26. The ^{13}C NMR spectrum of **6** in CD_2Cl_2.

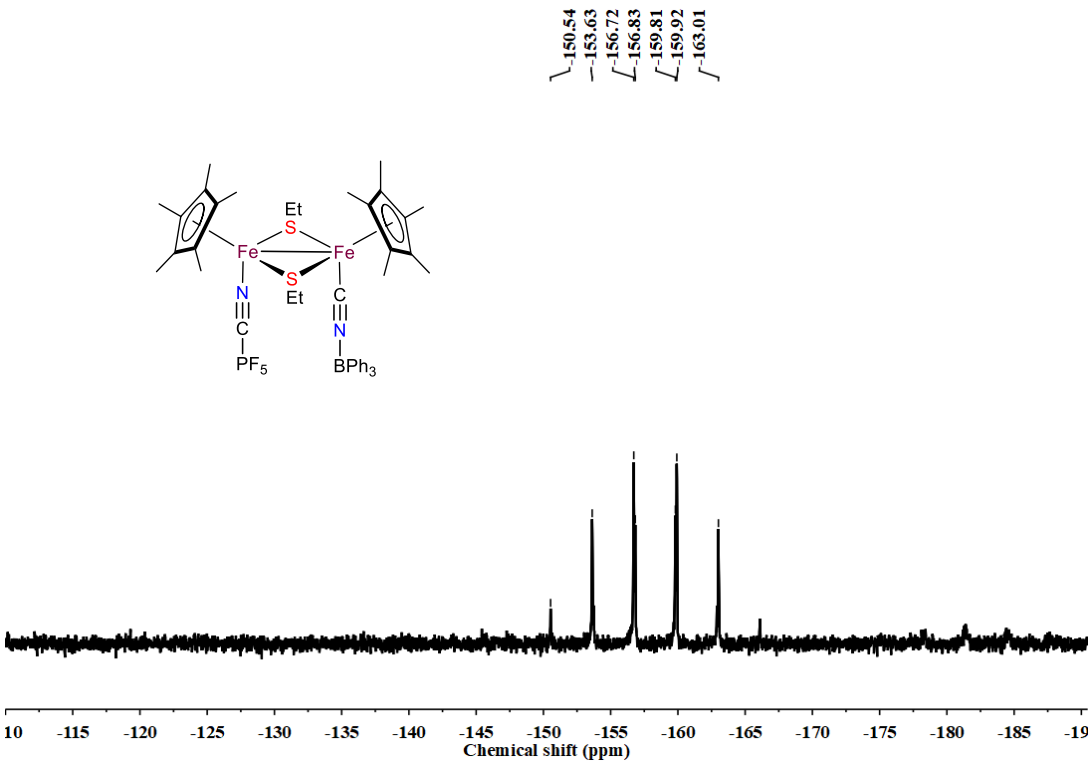

Figure S27. The ^{31}P NMR spectrum of **6** in CD_2Cl_2.

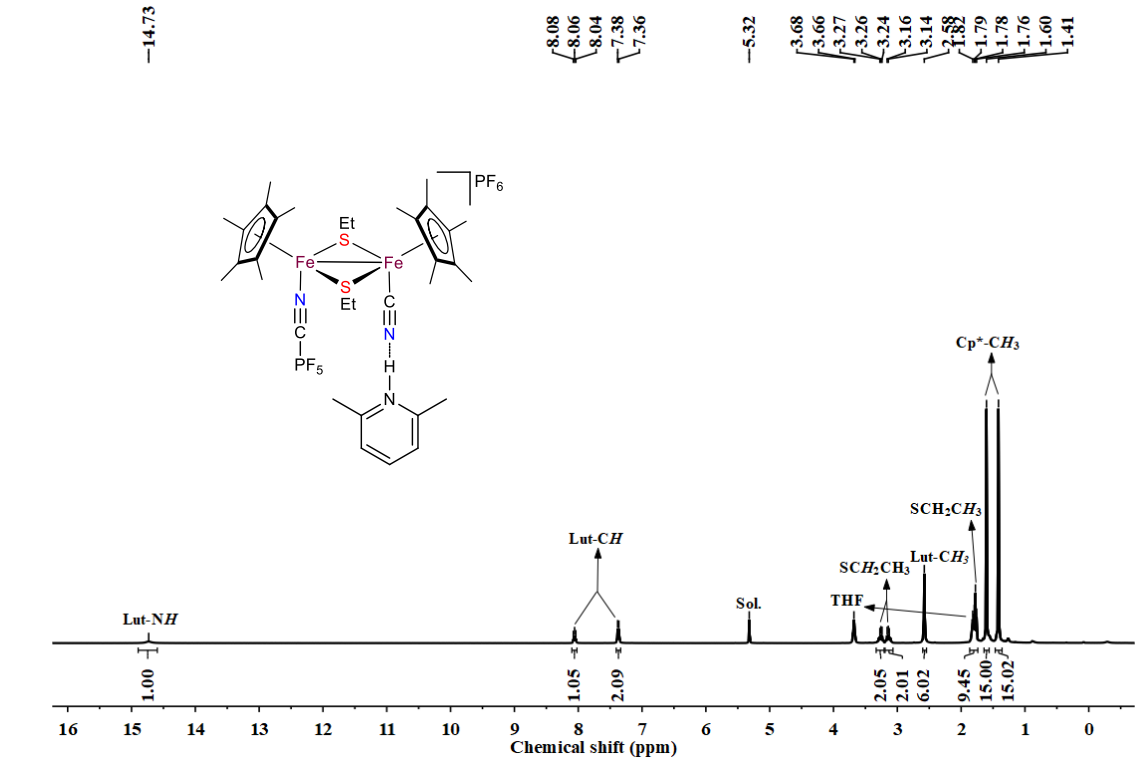

Figure S28. The ^{1}H NMR spectrum of **7** in CD_2Cl_2.

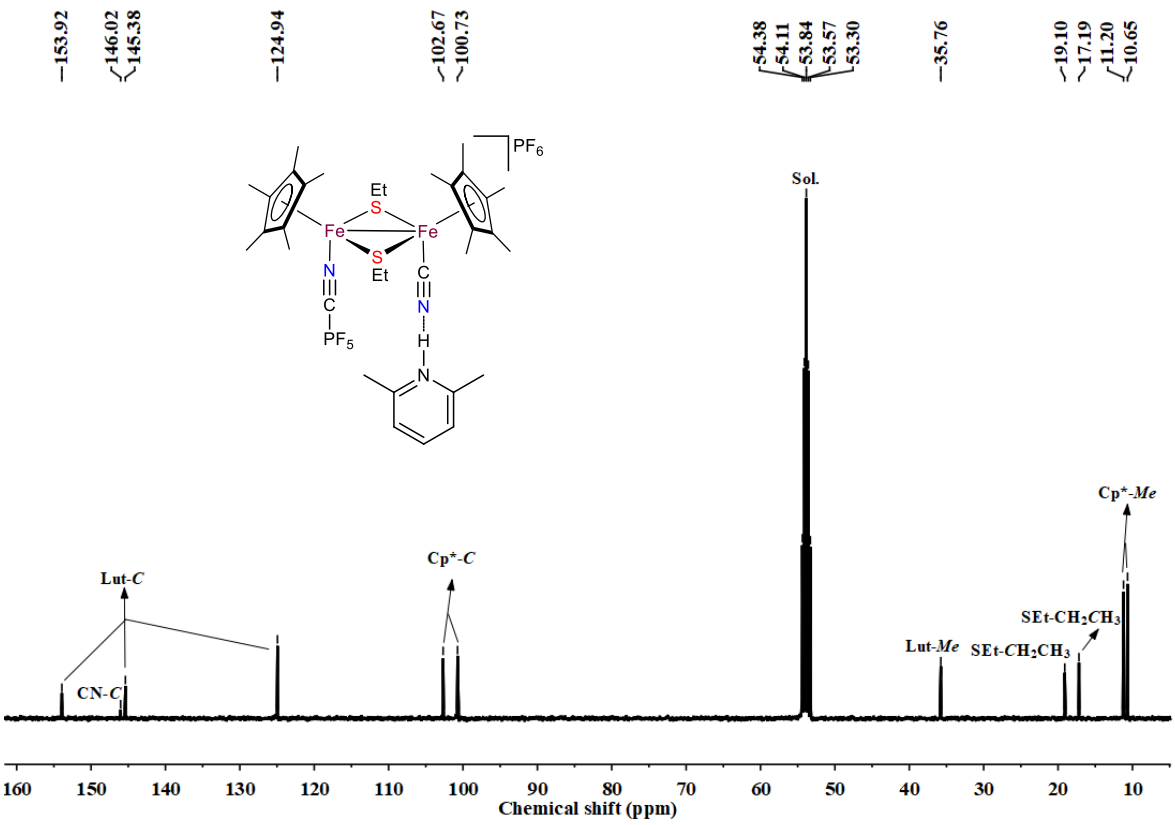

Figure S29. The ^{13}C NMR spectrum of **7** in CD_2Cl_2.

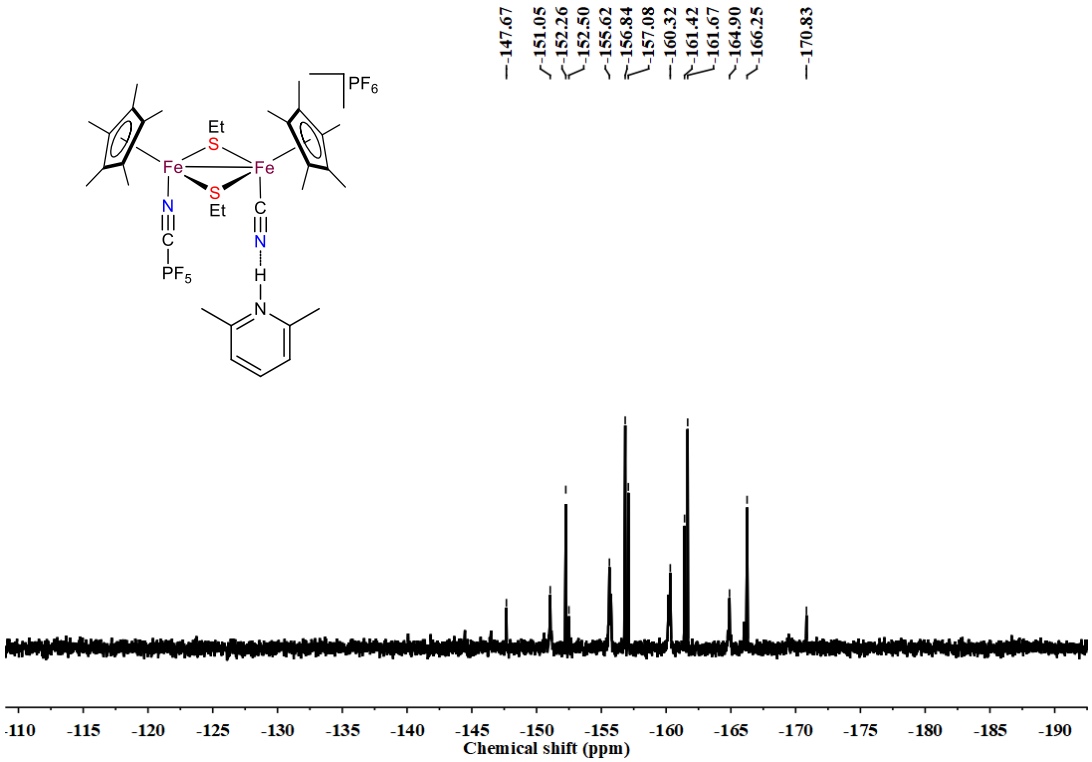

Figure S30. The ^{31}P NMR spectrum of **7** in CD_2Cl_2.

IV. IR spectra

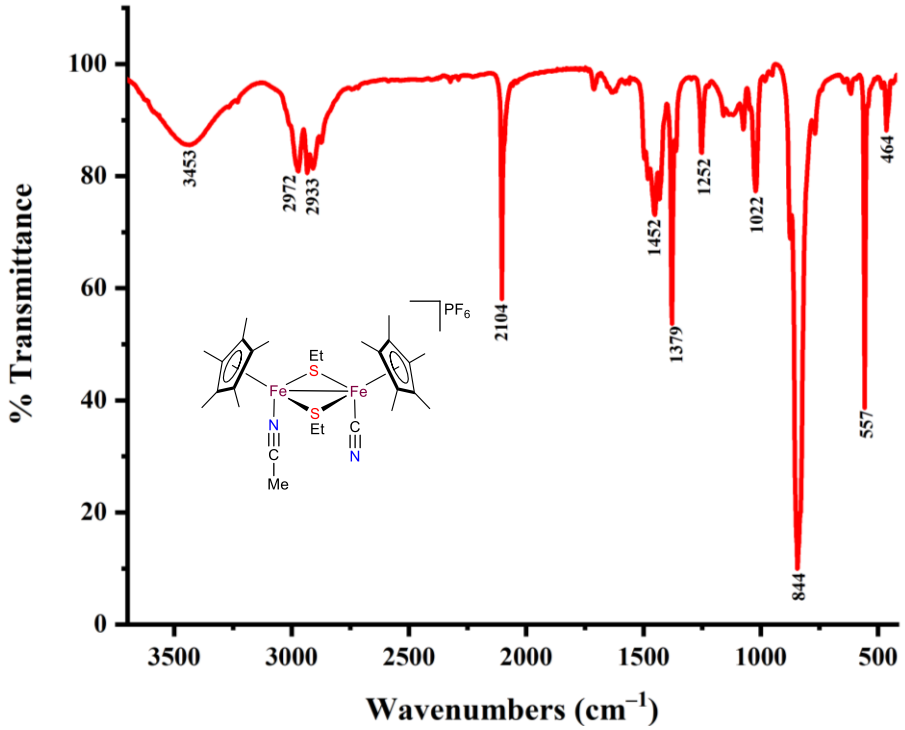

Figure S31. The IR (KBr) spectrum of **2**.

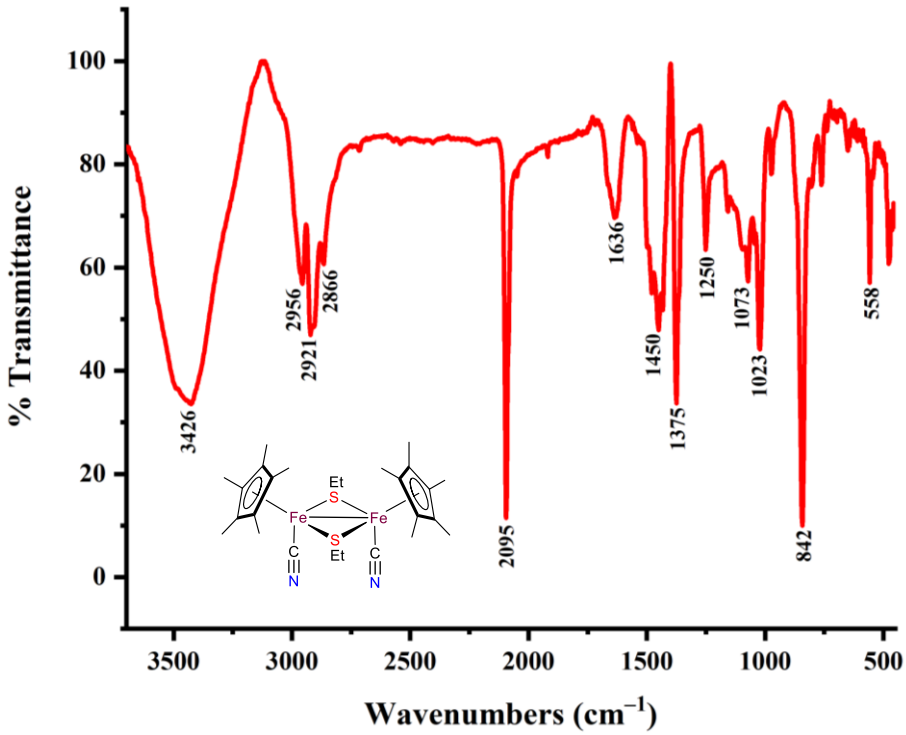

Figure S32. The IR (KBr) spectrum of **3**.

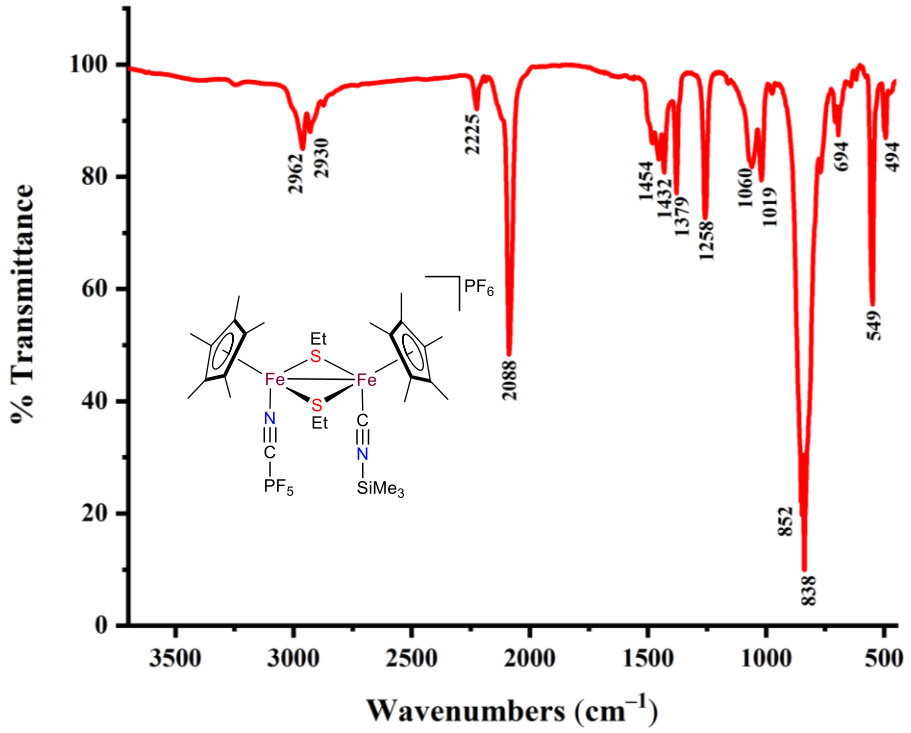

Figure S33. The IR (KBr) spectrum of **4**.

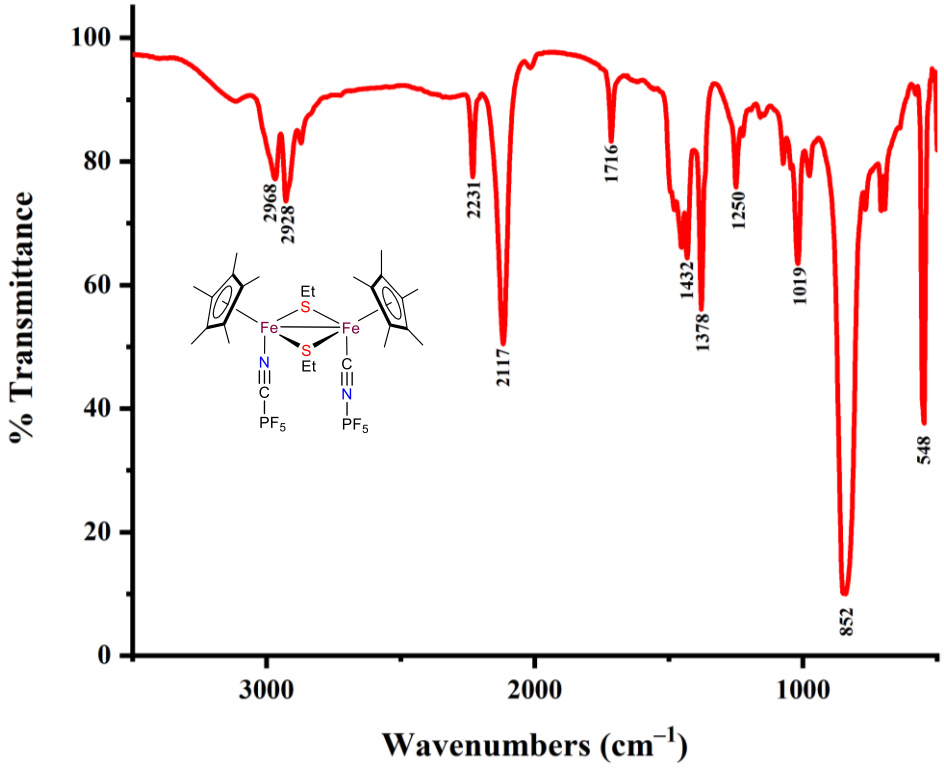

Figure S34. The IR (KBr) spectrum of **5**.

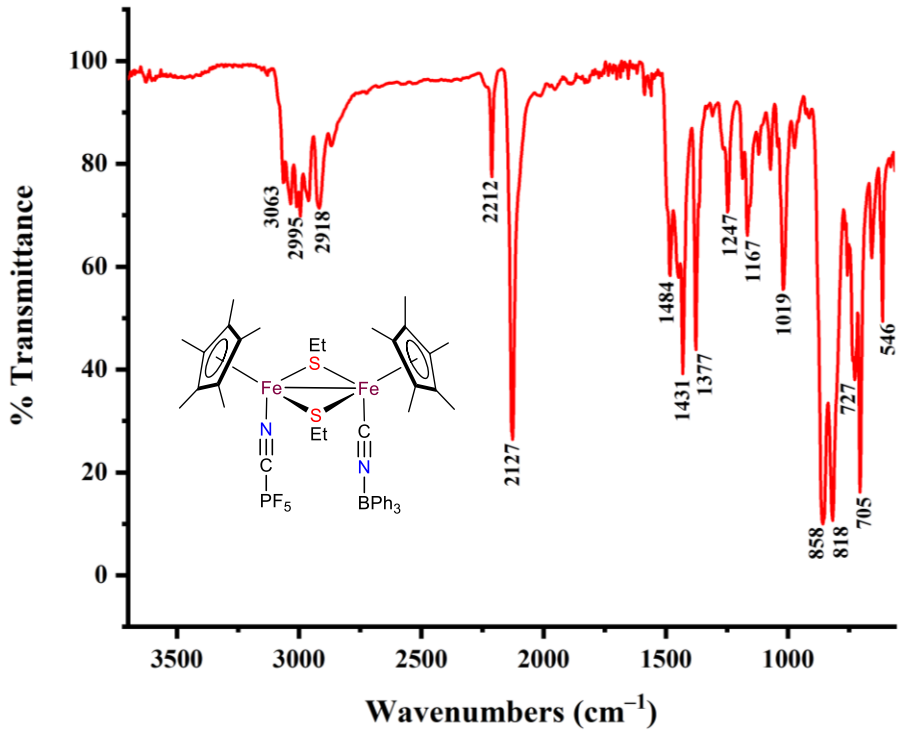

Figure S35. The IR (KBr) spectrum of **6**.

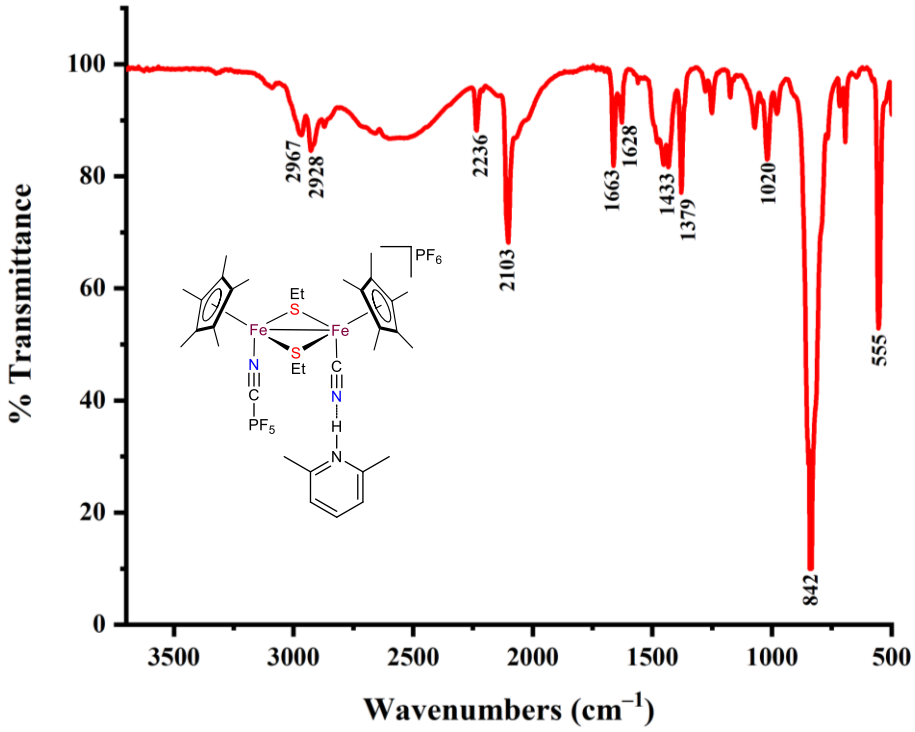

Figure S36. The IR (KBr) spectrum of **7**.

IV. *In situ* infrared spectra

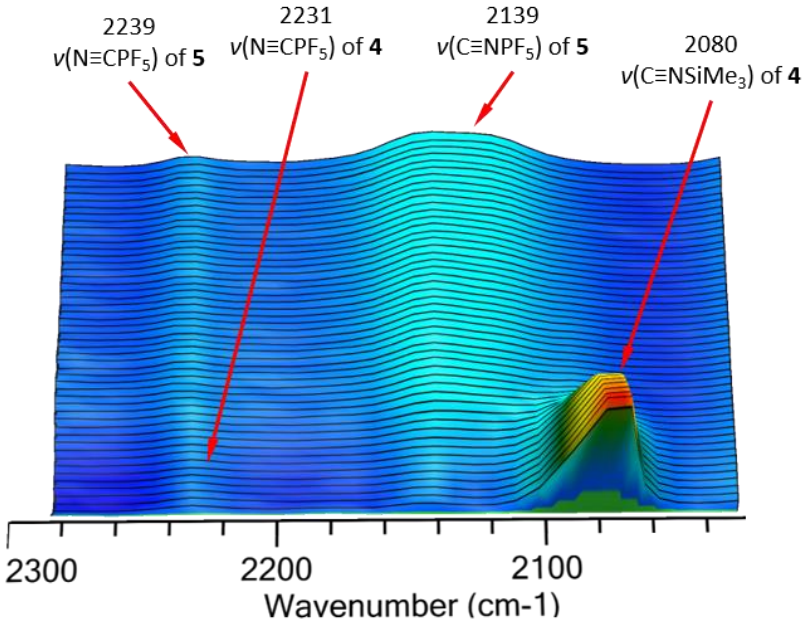

Figure S37. *In situ* infrared plot recorded at room temperature showing the formation of **5** from **4** in acetone.

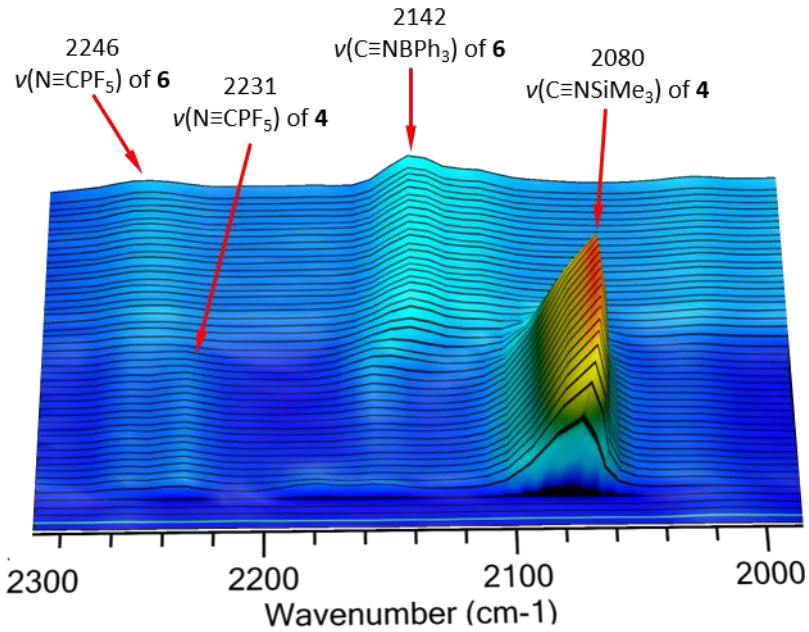

Figure S38. *In situ* infrared plot recorded at room temperature from the reaction of **4** with 1 equivalent of $NaBPh_4$ in CH_2Cl_2.

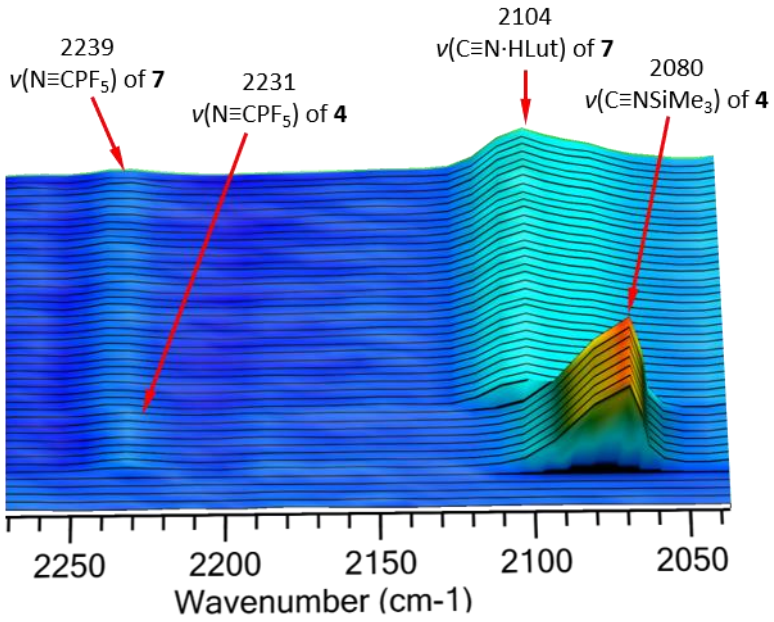

Figure S39. *In situ* infrared spectra showing the formation of complex **7** from the reaction of **4** with 1 equivalent of Lut·HCl.